Chemical Physics 24 (1977) 311–325
© North-Holland Publishing Company

VIBRATIONAL SPECTRA OF TRANSITION METAL HEXAFLUORIDE CRYSTALS. III. EXCITON BAND STRUCTURES OF MoF_6, WF_6 AND UF_6 *

E.R. BERNSTEIN and G.R. MEREDITH**
Department of Chemistry, Colorado State University, Fort Collins, Colorado 80523, USA

Received 11 March 1977

In this final paper in the series we present the overall vibrational band structure of MF_6 crystals based on the previously discussed two-particle, heavily doped mixed crystal, and neat crystal data, in addition to dilute mixed crystal studies. Calculations of ν_2 and ν_5 bands based on a quadrupole–quadrupole intermolecular interaction model are determined to be in substantial agreement with the observations. The ν_1 bands are discussed in detail for a series of concentration studies and it is possible to demonstrate that MoF_6 and WF_6 conform to the ideal mixed crystal model whereas crystals containing UF_6 do not. A consistent picture of gas-to-crystal shifts, resonance interactions, band shapes and structures, densities of exciton states, Fermi resonance, and simple multipolar interaction models emerges from these studies.

1. Introduction

In the two preceding papers [1,2] the Raman spectra of neat Mo, W, and UF_6 crystals were discussed and the structure of the overtone and combination Raman bands was investigated. In this paper we will analyze each of the exciton bands corresponding to the octahedral molecule normal modes of vibration in as much detail as possible. We are motivated in this phase of the investigation by an interest in the nature and magnitude of the intermolecular forces in the ground electronic state. Optical spectra of paramagnetic ReF_6 and IrF_6 evidence several important differences in these various host crystals [3,4]; it is suspected that host systems play a major role in pair-exchange couplings. Host systems also contribute significantly to spectra of guest molecules in the form of numerous intense two-particle features (guest electronic transition and ground state host vibration). Moreover, the two-particle states do not fall into the usual classification schemes. It is believed that these phenomena are intricately related to the somewhat different intermolecular interactions that arise in these inorganic molecular solids.

In addition to the $k = 0$ structure of these bands in neat crystals, mixed crystal data will be used to obtain site information and crude band structures, to identify origins of $k = 0$ structure, and to obtain information on the dispersion near $k = 0$. Approximate densities of states from two-particle bands of neat crystals and electrostatic multipole calculations for the ν_2 and ν_5 bands will also be employed to elucidate the intermolecular interactions.

Inherent in this analysis is the concept of an ideal mixed crystal [5]. In this limit, the substitution of one molecular type by another at a particular site in the crystal would cause no change in interactions between molecules but would simply remove the possibility of resonant energy transfer between the different type molecules. Initially these hexafluoride systems would appear promising in this regard because the crystal structures are very similar and there are significant differences in molecular vibrational frequencies. However, one must be aware that the differences in these frequencies are by and large not associated with an isotope-like effect. Only the ν_3 vibration includes a significant motion of the central metal atom. The changes are largely consequences of the different electronic properties of the molecules. As will be shown, the MoF_6 and WF_6 systems have similar

* Supported in part by ARO-D and ONR.
** Present address: Department of Chemistry, University of Pennsylvania, Philadelphia, PA 19174, USA.

intermolecular interactions. However, in the UF_6 crystal, presumably due to the presence of f orbital character in the molecule, the intermolecular interactions are somewhat different. Consequences of these differences will be discussed.

There are some interesting phenomena in the mixed crystal series which can be discussed in light of existing binary mixed crystal theory [5]. The theory is quite restrictive in the cases for which quantitative predictions exist. Preservation of crystal structure and equality of resonance transfer integrals limits strictly valid discussion to modes of WF_6/MoF_6 mixed crystals. For this series, comparisons must be made only on a mode-by-mode basis.

Finally, a summary of conclusions about the neat crystal Raman spectra [1,2] is in order as justification for division of the discussion of the series of vibrational bands according to molecular vibrational label rather than chemical identity: (1) the reduction of molecular symmetry in the crystal allows Raman scattering intensity for all molecular vibrations. The differences of relative intensities in the spectrum of each compound appears to be controlled by crystal and molecular Fermi resonances; (2) the $k = 0$ structure observed in UF_6 frequently spans roughly twice the width of the MoF_6 or WF_6 structure. The larger electronic polarizability of UF_6 is correlated with this fact; and (3) the $k = 0$ structures, though on different energy scales, are extremely similar if allowance is made for overlapping bands.

2. Theory

2.1. Mixed and neat crystals

A number of recent reviews exist on the subject of excitons in molecular crystals [5–8]. Using the frozen lattice approximation (neglect of external molecular motions) the crystal hamiltonian is (in the tight binding approximation)

$$\mathcal{H} = \mathcal{H}^0 + \mathcal{H}', \tag{1}$$

in which

$$\mathcal{H}^0 = \sum_{nq} \mathcal{H}^0_{nq} \tag{2}$$

is the sum of site adapted molecular hamiltonians for the Z sites indexed by q in the N unit cells indexed by n. The intersite hamiltonian is assumed to be the sum of all pairwise terms

$$\mathcal{H}' = \frac{1}{2} \sum_{nq \neq n'q'} V_{nq,n'q'}. \tag{3}$$

The conventional solution scheme is to assume an orthonormal localized basis which diagonalizes each $\mathcal{H}^0_{nq}$ separately. This basis is transformed into one-site exciton functions which transform irreducibly in the translational subgroup of the crystal space group and which diagonalize the Z operators ($\mathcal{H}^0_q = \Sigma_n \mathcal{H}^0_{nq}$). Finally, $\mathcal{H}$ is diagonalized in a limited space of these functions. These spaces usually are restricted to single excitation functions derived from one isolated molecule level. In general, $\mathcal{H}^0_{nq}$ yields either site or molecular energies e^f_0 (depending on the degree of approximation employed) and $\mathcal{H}'$ gives rise to both diagonal D^f (static) and off-diagonal (resonance or dynamic) crystal terms.

In order to use this model it is often convenient to have the static crystal terms included in $\mathcal{H}^0$ so that $\mathcal{H}'$ will be traceless in the appropriate space. An ideal dilute mixed crystal would then have guest excitation energies equal to those generated by $\mathcal{H}^0_{nq}$ for the corresponding neat crystal of the guest. In other treatments the operator $\mathcal{H}^0_{nq}$ may be different for the same molecule in mixed or neat crystals due to different effective site potentials.

The theory of disordered molecular crystals is typically applied to isotopic mixed crystals [5]. The assumptions made are: (1) the lattice is conserved – only substitutional disorder occurs; (2) only the static (site) interactions may vary, while the dynamic resonance exchange interactions are unchanged; and (3) the site symmetry is not effectively altered. It is conventional to write the site excitation energies for the fth excited state as $e^f_0 + D^f$ with e^f_0 being the site (or often the molecular) energy and D^f being the static crystal interactions. In this case a more stringent condition than (2) can be imposed (ideal mixed crystal); only e^f_0 may change from molecule to molecule but the static interactions D^f remain constant in the various crystals.

Letting e^f_A and e^f_B be the site excitation energies, a convenient parameter is

$$\Delta^f = e^f_B - e^f_A, \tag{4}$$

with an energy scale defined such that

$$\tfrac{1}{2}(e_A^f + e_B^f) = 0. \quad (5)$$

The virtual crystal local energy is then defined to be

$$\bar{e}^f = C_A e_A^f + C_B e_B^f, \quad (6)$$

where C_A and C_B are concentrations of the species A and B which constitute the mixed crystal. Using a configurationally averaged Green's function to describe binary disordered crystals and the method of moments (self-consistent expansion of the averaged Green's function) to express this operator, various relationships have been obtained for a number of limiting cases. Specific results concerning appropriate moments will not be given here but will be presented as needed.

A classification scheme for the mixed crystal band of interest has been developed and sets of restrictions have been delineated. Letting W be the total bandwidth and requiring Δ^f to be positive, the limits are [5]:

(1) Atomic limit: $\Delta^f > W, \quad W \to 0.$ (7)

(2) Separated bands: $\Delta^f > W.$ (8)

(3) Persistent case: $C_A C_B (\Delta^f)^2 \geqslant \mu_2^0, \quad \Delta^f < W.$ (9)

(4) Incipient bandgap: $C_A C_B (\Delta^f)^2 \lesssim \mu_2^0.$ (10)

(5) Amalgamation limit: $\Delta^f \ll W.$ (11)

In the above $\mu_n^0 = \int \rho^0(E) E^n \, dE$; $\rho^0(E)$ is the neat crystal density of states of the pertinent band.

2.2. Band calculations

A quadrupole–quadrupole interaction was used to model the ν_2 and ν_5 exciton bands. Calculation has been restricted to these features for a number of reasons: the best, most complete series exciton data can be obtained for them; ν_2 (e_g) and ν_5 (t_{2g}) transform as the quadrupole components $\{2^{-1/2}[Y_2^2 + Y^{-2}], Y_2^0\}$ and $\{2^{-1/2} e^{-i\pi/4}[Y_2^1 - iY_2^{-1}], -i2^{-1/2}[Y_2^2 - Y_2^{-2}], 2^{-1/2} e^{i\pi/4}[Y_2^1 + iY_2^{-1}]\}$, respectively; quadrupole moment sums converge quickly and unconditionally; dipolar bands (ν_3, ν_4) involve slowly converging sums and additional possible complications due to polaritons [9]; and the calculations require only a few empirical parameters. Specifically, for ν_2 we employed a site splitting parameter and a value of the quadrupole derivative for the actual ν_2 motion; for ν_5, two site parameters, a mixing parameter, and the quadrupole derivative for the ν_5 motion are in principle needed. In fact, the ν_5 mode and band structure are not particularly sensitive to the mixing and one of the site parameters. Motions in the ν_2 and ν_5 coordinates were assumed to induce quadrupole moments linearly.

Local coordinate systems for each site were constructed to ensure proper phasing of the sites and the second rank tensor components. The interaction energy, matrix elements of $V_{nq,n'q'}$, is then calculated out to 16 Å by a multipole expansion of the two charge distributions involved. Interactions of each molecule with 156 neighbors are thereby generated; the summation is constant to within better than 3% upon changing the interaction radius from 14 to 16 Å. To calculate band structures and densities of states, the completely positive octant (smallest non-redundant volume) of the Brillouin zone was used. The octant was divided symmetrically into 125 units for ν_2 and 64 units for ν_5. The hamiltonian was diagonalized for k values at the centers of these units. A more complete discussion and description of the calculational procedures can be found in ref. [10].

3. Experimental

Details of crystal preparation and Raman apparatus may be found in refs. [1–3,10]. It should be commented that some care was taken in calibrating the monochromator (and to include periodic drivescrew errors) so that absolute frequencies are believed accurate to at least ± 0.2 cm^{-1} for sharp features (the calibration curve was highly overdetermined). Precision and reproducibility have been observed at better than 0.05 cm^{-1} and thus relative shifts of transition frequencies within a limited range are known quite accurately.

4. Results and discussion

4.1. ν_1 bands

The breathing mode (ν_1) is expected to have negligible dynamic (exciton or resonance terms) or static (D terms) interactions in these crystals. Since neat and dilute mixed crystal spectra are quite sharp

(fwhh < 1 cm^{-1} typically), changes in crystal site potential can be readily observed. In this section validity of the ideal mixed crystal concept will be explored for the XF_6 crystal system. It will be shown that the ideal mixed crystal approximation is a useful approach to WF_6, MoF_6 and (by implication) other 4d and 5d, mixed crystal systems, but is inadequate for mixed crystals involving UF_6.

Table 1 provides a summary of the observed ν_1 peaks in the various crystals. ReF_6 data is also summarized there for a general comparison and completeness. The WF_6/MoF_6 series displays small monotonic shifts of the frequencies. The MoF_6 ν_1 feature ($\approx$742 cm^{-1}) moves to lower energy and the WF_6 ν_1 feature ($\approx$772 cm^{-1}) moves to high energy with increasing dilution. This is the prediction of the *separated band* approximation. However, the prediction of shifts, in this instance given by,

$$E_A = \epsilon_A^f - C_B\mu_2^0/\Delta,$$
$$E_B = \epsilon_B^f + C_A\mu_2^0/\Delta, \quad (12)$$

with $\Delta \approx 30$ cm^{-1} and $\mu_2^0 \leqslant 1$ cm^{-2}, cannot come close to an explanation for the relatively large (≈ 0.5 cm^{-1}) shifts found for MoF_6. Other effects could contribute to the observed shifts: small changes in static interaction terms with dilution; other levels of WF_6 interacting with the MoF_6 ν_1 level; or possibly other exciton branches associated with ν_1 (e.g., u-branches) induced by increased crystal doping, as evidenced by line shape changes. Notice, however, that shifts of ν_1 WF_6 are almost a factor of five greater in UF_6.

Table 1
ν_1 Raman frequencies in various crystals near 77 K

System	Energy (cm^{-1})	FWHH [a] (cm^{-1})
MoF_6	742.19	0.30
95% MoF_6/5% WF_6	742.15	0.35 [b]
50% MoF_6/50% WF_6	741.84	0.38
WF_6	772.25	0.28
50% WF_6/50% MoF_6	772.32	0.47 [c]
5% WF_6/95% MoF_6	772.40	0.44
95% WF_6/5% UF_6	772.56	0.37 [d]
50% WF_6/50% UF_6	771.94	0.78 [c]
10% WF_6/90% UF_6	770.32	0.78
5% WF_6/95% UF_6	770.14	0.63 [b]
UF_6	663.96	0.52
95% UF_6/5% WF_6	664.11	0.63 [b]
90% UF_6/10% WF_6	664.65	0.80 [e]
50% UF_6/50% WF_6 [f]	666.92	1.49
5% UF_6/95% WF_6 [f]	667.35	0.89
ReF_6	755.32	0.65
1% ReF_6/99% MoF_6	755.36	0.55
5% ReF_6/95% TeF_6	755.44	0.69
5% ReF_6/95% UF_6	752.78	0.91
99% MoF_6/1% ReF_6	742.26	0.31
95% UF_6/5% ReF_6	663.89	0.60

a) These values are measured from spectra with slit widths of 0.2 cm^{-1}.
b) Peak is noticeably asymmetric with high energy broadening.
c) Peak is noticeably asymmetric with low energy broadening.
d) Peak has a significant tail on the low energy side.
e) Peak has a significant tail on the high energy side.
f) Similar behavior was observed in UF_6/MoF_6 mixed crystals. Energies for heavily doped and dilute crystals were 665.6 (3.5 cm^{-1} fwhh) and 668.1 cm^{-1} with low energy broadening of 665.6 cm^{-1} peak.

The shifts of UF_6 ν_1 in the WF_6/UF_6 series are large and in the direction of the WF_6 ν_2 band centered at 675 cm^{-1}. This observation indicates changes in the static (D term) interactions. Further support for this conclusion is found in the fact that the energy of ν_1 of UF_6 in WF_6 increases and the energy of ν_1 of WF_6 in UF_6 decreases in increased dilution. The increased line widths with increased dilution are indications of inhomogeneous broadening due to the variety of site potentials possible, depending on the assortment of WF_6 and UF_6 neighbors. An extreme possibility is that local lattice distortions may occur due to differences of interactions between neighboring molecules. Clearly, though, there is no exclusion occurring despite literature reports of solid–solid phase separations at intermediate mole fractions [11,12]. These studies dealt with solid–liquid equilibria while our crystals were vapor phase grown at temperatures below both the triple-point and solid–solid phase transition point.

Table 1 also contains comparable data on ReF_6 neat and mixed crystal to indicate that similar ideal mixed crystal trends are followed even in the presence of exchange forces associated with paramagnetic species [3]. The Jahn–Teller nature of this system [13] apparently plays a minor role in these considerations.

Referring to the vapor phase frequencies in table 2, gas-to-crystal shifts (D terms) are very small for WF_6 and MoF_6. However, the approximately 3 cm^{-1} shift

Table 2
Vapor phase transition frequencies (in cm^{-1})

	ν_1	ν_2	ν_3	ν_4	ν_5	ν_6
MoF_6 a)	741.8	652.0	741.1 d)	264	317	117
WF_6 b)	772.1	678.2	712.4	252.1	320	129
UF_6 c)	667	534	625.5	186.2	200.4	143

a) Ref. [14]. b) Ref. [15]. c) Ref. [16]. d) Ref. [18].

(assuming no $k = 0$ shift) of UF_6 in UF_6 compared to $\approx 0\ cm^{-1}$ shift of UF_6 in WF_6 is probably significant. This difference is most likely associated with the increased molecular distortion in UF_6 crystal.

To recapitulate, due to the small exciton interactions for ν_1 modes, it has been possible to determine that the static crystal interactions are small for WF_6 and MoF_6 crystals (even for dilute mixed crystals with UF_6 guests). However, in UF_6 crystals the static terms are appreciable with respect to the other members of this series.

4.2. ν_2 bands

The bands corresponding to the molecular ν_2 fundamental offered the greatest possibilities for complete interpretation due to the limited degeneracy and strong Raman scattering. The neat crystal spectra were presented in fig. 3 of paper I [1] and are summarized here in table 3. The mixed crystal spectra are displayed in figs. 1, 2, 3, and 4. The site energies of the two components (A′ and A″ on the C_s site) of the split vibrations are summarized in table 3. Despite the static effects of the WF_6/UF_6 series mentioned in the last subsection, the WF_6 ν_2 centers of gravity in UF_6 and MoF_6 differ by less than 0.1 cm^{-1}. This probably arises from a cancellation of negative static and positive pseudoresonance contributions. Rough estimates of these latter second-order terms ($\approx 5\ cm^{-1}$) are in agreement with a balancing of the two effects.

Table 3
Summary of ν_2 and ν_5 Raman $k = 0$ band structures of neat crystals. The raw data comes from tables 2, 3 and 4 of paper I. The $k = 0$ components are normalized to give top and bottom component reduced energies of 1 and 0

Crystal	Width of $k = 0$ structure (cm^{-1})		Normalized $k = 0$ energies	
	ν_2	ν_5	ν_2	ν_5
UF_6	23.6	22.9	1.000	1.000
			0.318	0.846
			0.259	0.389
			0.000	0.196
				0.000
WF_6	9.7 a)	8.0	1.000 a)	1.000 b)
			0.662	0.416
			0.458	0.000
			0.309	
			0.000	
MoF_6	10.0	8.7	1.000	1.000 b)
			0.319	0.401
			0.269	0.000
			0.000	

a) Overlaps with ν_3 band, structure somewhat distorted and extra feature generated. See text and paper I [1] for further discussion.
b) Not well resolved peaks.

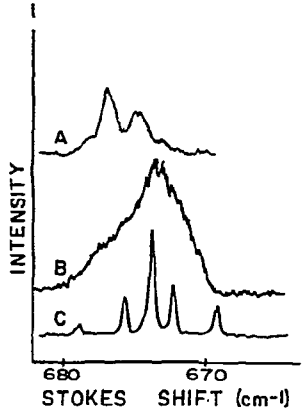

Fig. 1. Raman spectra of the ν_2 region of WF_6 in various crystals near 77 K. (A) 5% WF_6 in MoF_6. (B) 50% WF_6 in MoF_6. (C) Neat WF_6.

The site splittings for the WF_6 ν_2 vibration are, however, quite different: 3.9 cm^{-1} for WF_6 in UF_6 and 2.1 cm^{-1} for WF_6 in MoF_6. Comparing these numbers with the observed 2.4 cm^{-1} site splitting of UF_6 in WF_6, one concludes that the ν_2 site splitting for UF_6 in UF_6 is greater than 4 cm^{-1} and about equal to 2 cm^{-1} for WF_6 in WF_6. Since the $k = 0$ structure approximately brackets the total bandwidth (see below), these splittings are $\approx 20\%$ of the total bandwidths. Using this value (with the A′ component higher than the A″ component as predicted in the

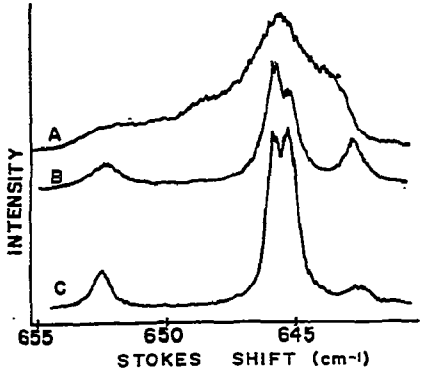

Fig. 2. Raman spectra of the ν_2 region of MoF_6 in various crystals near 77 K. (A) 50% MoF_6 in WF_6. (B) 5% WF_6 in MoF_6. (C) Neat MoF_6.

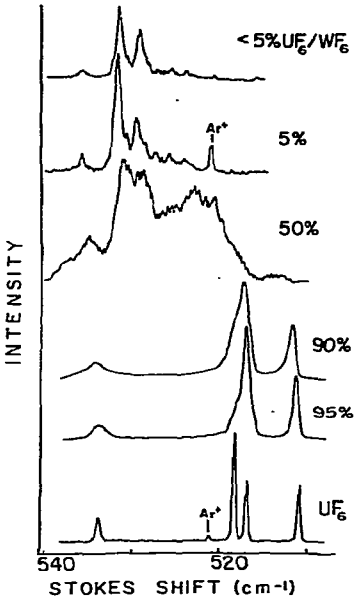

Fig. 3. Raman spectra of the ν_2 region of UF_6 in various crystals near 77 K. An 80% UF_6 with WF_6 mixed crystal spectrum is also shown in fig. 1 of paper II [2]. The features marked Ar^+ are the 5287 Å laser plasma line. Some of the concentrations have been achieved by examining the ends of crystals where the kinetic process of vapor to crystal growth and the large differences in vapor pressure of WF_6 and UF_6 have created concentration gradients.

D_{4h} model) in a quadrupole–quadrupole calculation of the exciton structure, a density of states curve matching the observed $\nu_1 + \nu_2$ two-particle band structure (paper II [2]) obtains. Not even qualitative agreement is found if the A″ component is placed higher or if site splitting is omitted [10]. This calculation predicts the site energy center of gravity (also the band center of gravity for an isolated band) to be at 0.651 when the band is normalized on the $k = 0$ structure (as in tables 3 and 4).

Referring to the data of table 2, the averaged gas-to-crystal shifts are −2.5 and −3.2 cm^{-1} for WF_6 in MoF_6 or UF_6 and UF_6 in WF_6. Using a value of −2.5 cm^{-1} as a guess for D of MoF_6 in MoF_6, 649.5 cm^{-1} (a normalized value of 0.71 in the band) would be the site energy center of gravity. The apparent inconsistency for UF_6 in WF_6 versus the neat crystal band centers can be rationalized on the basis of the afore-

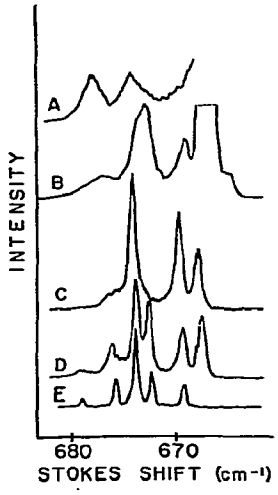

Fig. 4. Raman spectra of the ν_2 region of WF_6 in various crystals near 77 K. (A) 5% WF_6 in UF_6. (B) 50% WF_6 in UF_6. (C) 5% UF_6 in WF_6. (D) < 5% UF_6 in WF_6. (E) Neat WF_6. The peak in the 664 to 668 cm^{-1} region is the ν_1 peak of UF_6. In (B) the shoulder around 665 is UF_6 ν_3 structure. This band is complicated due to the overlap of the ν_2 and ν_3 WF_6 structures.

mentioned pseudoresonance and static shift terms which lower the band center to ca. 0.7. Thus, all estimates of the band centers of gravity are in rough agreement, implying that all interactions are scaled proportionally in this band.

The quadrupole–quadrupole calculation predicts $k = 0$ (normalized) energies and factor group (D_{2h}) symmetries at 0 (A_g), 0.250 (B_{1g}), 0.483 (B_{2g}) and 1.000 (B_{3g}) in reasonable agreement with data in table 3. The finer atom–atom interaction ignored may in fact invert the ordering of the B_{1g} and B_{2g} components.

By comparing mixed crystal behavior with calculated dispersion curves, the details of the calculated structure may be tested. All of the mixed crystal series show a significant rise of the lowest energy component with the addition of small amounts of dopant. The relaxation of strict k selection rules allows transitions to states in the region $k \approx 0$ of the Brillouin zone. The rise indicates definite upward dispersion in agreement with all calculated dispersion curves [10]. Thus $k = 0$ occurs at the bottom of the band. The amalgamation of the inner two components with negligible shift also agrees with the relative dispersion of these branches in all calculated dispersion curves. The upper branch, in the calculation, has weak upward dispersion in the b and c directions, but strong downward dispersion in the a direction. This fits the behavior of small shift but increased width (compared to the other components) in the Raman spectra. The $k = 0$ structure occurs near, but not at, the top of the band; its width, therefore, is only an approximation to the total exciton bandwidth.

It is interesting that the g, u character of the branches seems to be retained after $k = 0$ selection

Table 4
Summary of observed ν_2 and ν_5 Raman spectra in dilute mixed crystals

Guest	Host	Vibration	Gas phase energy (cm^{-1}) b)	Energy (cm^{-1})	FWHH (cm^{-1})	Center of gravity (cm^{-1})	Normalized center of gravity a)
UF_6	WF_6	ν_2	534	529.56 531.96	1.0 0.85	530.76	0.847 c)
		ν_5	200.4	204.5	2.8	204.5	−0.097 d)
WF_6	UF_6	ν_2	678.2	673.7 677.6	2.8 2.5	675.7	0.669
		ν_5	320	321.6	5.1	321.6	0.157 d)
WF_6	MoF_6	ν_2	678.2	674.73 676.79	1.8 1.4	675.76	0.678

a) Normalized as in table 3.
b) See refs. [14–16].
c) See text, section 4.2.
d) See text, section 4.4.

rules have been destroyed. Branches which become ungerade at $k = 0$ do not appear in the spectra for small dopant concentrations. This is probably correlated with the fact that the dispersion of all of these nondegenerate branches must be zero at $k = 0$ (by spatial symmetry or by time reversal invariance).

Consulting tables 3 and 4 of paper I or the gas phase data, an approximate value of $\Delta \approx 27$ cm^{-1} (ignoring site splittings) is determined for MoF_6 and WF_6. Since $W \approx 10$ cm^{-1}, this is a separated-bands-disordered-mixed-crystal case provided there is no interference from other crystal bands. That is why the ν_2 bands of WF_6 and MoF_6 (figs. 1 and 2) retain their separate identities.

It has been shown here, that the ν_2 band structure for all three neat and mixed crystal systems is very nearly identical. A reasonably consistent picture of the ν_2 crystal properties and interactions emerges if the molecular properties of Mo, W, and UF_6 (e.g., polarizabilities) are considered. Interactions in crystals involving UF_6 in significant concentrations are typically 2.5 times larger than those in the MoF_6/WF_6 systems. The ν_2 $k = 0$ structure approximately brackets the band with the band center occurring ~ 70% of the distance into this structure. The gas-to-crystal shifts in this averaged band picture are roughly 20 to 30% of the total band width as are the site splittings.

4.3. ν_3 bands

The ν_3 Raman transitions are crystal induced and hence weak; consequently no dilute mixed crystal information could be obtained. The bands are also in a congested spectral region, as ν_3 falls between (and sometimes within) the regions of the more intense ν_1 and ν_2 transitions. Figs. 5 and 6 display the neat and mixed crystal series (see also fig. 5 of ref. [1]). The ν_3 structure of UF_6 in the UF_6/WF_6 mixed crystal series (fig. 6 of ref. [2]) has been compared to the two-particle structure of the $\nu_1 + \nu_3$ and $\nu_2 + \nu_3$ infrared absorption bands. Unfortunately, in MoF_6, the intense ν_1 transition hinders complete observation of the upper energy end of the ν_3 band. Nonetheless, the $k = 0$ structure of MoF_6 (fig. 6) is very much like that of the lower energy components in UF_6. Since the unobstructed, observed exciton width is ≈ 65 cm^{-1} in UF_6, one can scale the spacings of the lower $k = 0$ components of the neat crystals to arrive at an estimated exciton band for MoF_6 of $\approx 110\%$ that of UF_6. Presumably the corresponding higher energy components of MoF_6 ν_3 are masked in MoF_6 by ν_1. The

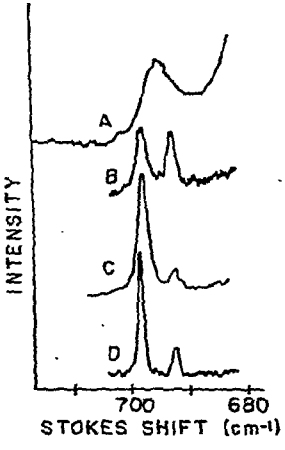

Fig. 5. Raman spectra of weak features to high energy of the intense ν_2 structure of WF_6 in various crystals near 77 K. These spectra are immediately adjacent to but lower in intensity than those of fig. 4. Neither structure is indicative of an isolated exciton band due to $\nu_2 - \nu_3$ crystal induced interactions. (See text.) (A) 50% WF_6 in UF_6. (B) 5% UF_6 in WF_6. (C) < 5% UF_6 in WF_6. (D) Neat WF_6.

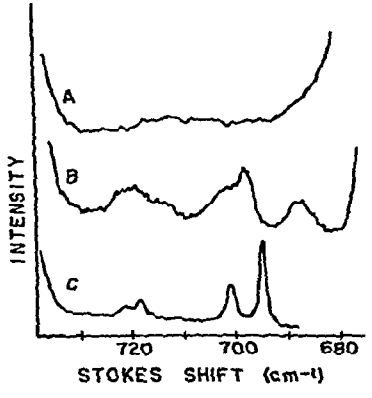

Fig. 6. Raman spectra of the ν_3 exciton region of MoF_6 in various crystals near 77 K. (A) 50% MoF_6 in WF_6. (B) 5% WF_6 in MoF_6. (C) Neat MoF_6. The feature at 688 cm^{-1} is due to WF_6 ν_3 (and ν_2). The sizeable intensity is discussed in the text. The rise at high energy is the MoF_6 ν_1 and at low energy is the WF_6 ν_2/ν_3. Very similar mixed crystal spectra of the ν_3 region of UF_6 are shown in fig. 6 of paper II [2].

Table 5
Summary of ν_3 and ν_4 Raman $k = 0$ band structures of neat crystals

Vibration	$k = 0$ component frequencies (cm^{-1})			Normalized or shifted $k = 0$ frequencies (cm^{-1})		
	WF_6	UF_6	MoF_6	WF_6	UF_6	MoF_6
			(247.62)			(−4.72) a)
ν_4	246.11	175.33	252.34	0	0	0
	249.87	185.83	261.87	9.76	10.50	9.53
		191.64	267.25		16.31	14.91
		197.18	272.08		21.85	19.74
	265.85		275.81	25.74		23.47
ν_3	a)	586.39	694.60	a)	0	0
		590.06	702.63		3.67	8.03
		608.43	718.73		22.04	24.13
		610.74	721.64		24.35	27.04
		649.08	b)		62.69	[≈70] c)

a) Overlapping band situation (see text).
b) Conjectured to be obscured by ν_1.
c) Extrapolated value (see text).

similarity of MoF_6 and UF_6 $k = 0$ structure is emphasized in table 5. In fact, further evidence for the similar band structure can be found in the behavior of both UF_6 and MoF_6 on addition of WF_6 dopant. (One must consider that the lower energy structure of the MoF_6/WF_6 mixed crystals is due to WF_6 ν_3 and ν_2.) Here as for ν_2, the low energy $k = 0$ component appears to be the bottom of the band. The WF_6 structure is not easily analyzed due to the overlap and mixing with the ν_2 band. The observed structure (fig. 5) does not resemble that of MoF_6 and UF_6.

The ν_3 band structure is most likely determined by electrostatic transition dipole–dipole interactions. The band width should then be proportional to the square of the transition dipole, as is the oscillator strength for infrared absorption. While apparently no oscillator strengths are available in the literature, the published spectra [17] give some idea of the relative strengths. The UF_6 ν_3 absorption maximum corresponds to 5.7×10^{-2} o.d./torr cm while in MoF_6 it is 6.8×10^{-2} o.d./torr cm. This comparison is only intended to show that there is qualitative agreement between the bandwidths and the transition dipole oscillator strengths.

The behavior delineated for ν_3 is certainly in contrast to that found for ν_2 and one can therefore conclude that each band carries its own interaction mechanism and that the scaling factors between crystals (MoF_6, WF_6, UF_6 neat crystals) must be determined for each band. In fact, we see here that the ordering of scaling factors has reversed for ν_3 compared to ν_2. However, there is still a correlation with the magnitude of the appropriate *molecular* properties.

The ν_3 gas phase frequencies (table 2) are 46.5 and 39.1 cm^{-1} above the lowest $k = 0$ components (approximately the bottom of the bands) in MoF_6 and UF_6; the actual gas-to-crystal shifts are difficult to extract due to the lack of dilute mixed crystal data and the incomplete band structure. If the values are normalized for bandwidths, they agree to within 5% of the bandwidth. Using MoF_6 parameters for WF_6 the bottom of an unperturbed band is predicted around 665 cm^{-1}, a value *lower* than the lowest observed $k = 0$ component in both the ν_2 and ν_3 structure. The ν_2/ν_3 overlap and mixing must be severe for this crystal.

A striking feature of the ν_3 exciton band further confirms these large exciton "dipolar type" interactions. Only the ν_3 and ν_4 modes have appreciable motion of the central metal. Natural uranium is greater than 99% ^{238}U, but natural molybdenum consists of seven isotopes all in roughly equal proportions [19]. The ν_3 gas phase frequency varies by 8.1 cm^{-1} between $^{100}MoF_6$ and $^{92}MoF_6$ [14]. Despite this spread of frequencies the $k = 0$ structure is sharp. This is a very complicated amalgamated band situation. The

resonance interactions override differences in site energies, creating a band structure apparently identical to that of an isotopically pure crystal.

In the MoF_6/WF_6 mixed crystal series (fig. 6) structure attributed here to WF_6 appears quite strong in relation to the MoF_6 ν_3 structure considering the relative concentrations. Possible explanations for this perturbation involve strongly interacting bands; WF_6 ν_3 levels may amalgamate with the MoF_6 band and/or WF_6 ν_3 levels may steal additional intensity from the intense WF_6 ν_2 transitions.

An infrared investigation of these regions would be interesting not only because the dilute crystals could be studied, but also because the nature of the WF_6/MoF_6 ν_3 amalgamation would be clearer due to the change of intensity mechanism.

The important conclusions from this section are: unperturbed ν_3 bands are dipolar in nature, band widths are large, and resonance interactions dominate the smaller site energy differences. As with ν_2 bands the gas-to-crystal shifts scale approximately with band interactions. The scaling between the same bands of different crystals is largely determined by the appropriate molecular parameter (i.e., polarizability, dipole moment, etc.).

4.4. ν_5 bands

ν_6, ν_4 and ν_5 comprise the crowded bending region of the spectrum and, to a greater or lesser extent in all crystals, these modes must be treated as interacting bands. The mixed crystal spectra become especially difficult to treat without prior expectations based on ν_2 and ν_3 data. The neat crystal spectra have been presented in paper I [1] (fig. 4 and tables 3, 4 and 5) and ν_5 density of states data are presented in paper II [2] (figs. 7 and 9). The similarity of the $k = 0$ structures for MoF_6, WF_6, and UF_6 is shown in table 3 and the dilute mixed crystal data are presented in table 4.

In general, the mixed crystal data do not contradict the previous conclusions of two-particle $\nu_1 + \nu_5$ spectra. The WF_6/MoF_6 series, and perhaps the other series as well, is a good example of an amalgamated band binary mixed crystal [5,10]. Because of these complications and additional spectral congestion, rather more than justifiable weight will be given to the quadrupole–quadrupole calculation in the band analysis.

Table 6
ν_5 exciton band centers extrapolated from $\nu_1 + \nu_5$ two-particle spectra. The computed ν_5 density of states was fit to the observed spectra and the ν_1 frequency was subtracted to give the ν_5 band center

Crystal	ν_5 band center (extrapolated from two-particle spectra and calculations)	Normalized band center [a]
UF_6	216.5	0.429
WF_6	323.6	0.407
MoF_6	320.0	0.458

[a] Normalized as in table 2.

The dilute mixed crystal values of table 4 do not agree well for the positioning of the site centers of gravity within the band structures. Consequently the calculated density of states function was positioned on the observed $\nu_1 + \nu_5$ two-particle structure and a center of the band (a value from the calculation) was determined. Subtracting the ν_1 frequencies gave the values listed in table 6. The normalized band position agree much better than the experimentally observed dilute crystal centers of gravity do. Moreover, in the physically reasonable regions of the site splitting space [10], the calculated band center falls close to the UF_6 $k = 0$ component with ($k = 0$ band) normalized value ≈ 0.39 in agreement with the extrapolated values. It thus appears that one need explain why the normalized dilute crystal values are significantly different than ≈ 0.40.

Dilute mixed crystal quasi- or pseudoresonance interactions have been calculated for ν_5 in various hosts employing eqs. (12). Four precautions must be borne in mind when applying such calculations to real systems: (1) excitonic interactions with overtones are weak since two vibrational quanta must be transferred. (Considering the intersite potential as an expansion in the site normal coordinates, the necessary terms are "higher order".); (2) the interaction parameters used in eqs. (12) are properties of the hosts. As discussed in the ν_1 section, however, the interaction is really dependent on both molecules, not just the host. Comparing widths of ν_5 bands, the UF_6 in WF_6 and WF_6 in UF_6 interaction matrix elements (μ_2^0 is related to the square of these) should be scaled by some factor, say the geometric mean of the ν_5 bandwidths. This increases the UF_6 in WF_6 shifts by a factor of 2.9 and

decreases the WF_6 in UF_6 shifts correspondingly; (3) the shift terms are not additive. Formally one should solve a simultaneous coupling problem, but this is probably not the most severe approximation made for this correction; and (4) the comparison to neat crystal band centers must take account of the interband interactions which shift the band center from the ideal mixed crystal position.

The main conclusion from these pseudoresonance calculations is that ν_5 of the WF_6 in UF_6 is probably perturbed by less than 1 cm^{-1} but the UF_6 in WF_6 ν_5 position is depressed by more than 10 cm^{-1}. Thus, the UF_6 neat crystal band center would be expected at ≈ 0.45 in substantial agreement with table 6 and the WF_6 data would remain unchanged.

If one accepts the band centers of gravity in table 6, gas-to-crystal shifts are 3.0, 3.6 and 16.1 cm^{-1} for MoF_6, WF_6 and UF_6 respectively (see table 2). The latter value appears out of line until one considers the proximity of both the ν_4 and ν_6 vibrational levels in UF_6. The larger C_s distortion of the UF_6 molecules in neat crystal undoubtedly destroys the true octahedral vibrational description and the ensuing crystal site Fermi resonance may push the "ν_5" vibration upward. Indeed, the ν_4 and ν_6 bands are more intense relative to the ν_5 mode in UF_6, than in the other systems. There is also the possibility of significant contributions from interacting band terms (off diagonal transfer integrals pushing the ν_5 band upward), although the similarity of WF_6, MoF_6 and UF_6 bands should be altered by this effect.

Another important factor in frequency changes from vapor to solid in this region is the shift of the $2\nu_6$ energy levels (see later discussion). On entering the solid, Fermi resonance between $2\nu_6$ and ν_5 should increase for both WF_6 and MoF_6, but decrease for UF_6. Since $2\nu_6$ is above ν_5 of UF_6, this will also contribute to an increase in the UF_6 ν_5 frequency. However, the positioning of these levels in the other two molecules should also create increase of the ν_5 frequency on entering the solid. While these arguments are all qualitative, they are corroborated by the observed upward (positive) gas-to-crystal shift.

In summary, we have shown that the ν_5 bands are indeed similar for all neat crystals and are mostly quadrupolar in nature, in rough agreement with calculations (see paper II [2]). The magnitudes of respective resonance interaction (tables 3, 4 and 6) scale qualitatively with expectations of molecular polarizabilities. Details of gas-to-crystal shifts are complicated by pseudoresonance host-guest interactions and crystal induced and altered Fermi resonances which contribute to the observed large positive ν_5 shifts.

4.5. ν_4 bands

The neat crystal spectra of the ν_4 bands are summarized in table 5. In MoF_6 and WF_6 the intense $2\nu_6$ band masks and possibly perturbs (but see below) the high energy portions. In UF_6 the ν_5 and ν_6 bands bracket the ν_4 structure and may also be masking and/or perturbing it. The above notwithstanding, by shifting the energy reference to the lowest corresponding $k = 0$ components (table 5) the similarity of the bands is portrayed. Vapor phase frequencies (table 2) for MoF_6, WF_6, and UF_6 occur 11.7, 12.0 and 10.9 cm^{-1} above the common reference components, again emphasizing a consistency of details.

As with the ν_3 band, exciton structure is probably determined largely via dipole–dipole interactions. The MoF_6 infrared absorption spectrum of Claassen et al. [20] and the UF_6 infrared absorption spectrum of Frlec and Claassen [21] and Burke et al. [17] give ν_3 to ν_4 peak height o.d. ratios of 3.2 and 5.0 agreeing (considering the crudeness of the gas phase oscillator strength ratio estimates) with the ratios of observed and extrapolated exciton bandwidths.

A comment should be made about the dissimilar structure observed at $k = 0$ for the two "dipole" bands. In a high symmetry crystal, all dipole–dipole bands would have the same structure but for a scaling factor (the square of the transition dipole moment). In the transition metal hexafluorides, site splittings occur and may be appreciable fraction of the width of the narrower bands. Consequently, since these splittings may vary from band to band, there is no requirement that bands with similar resonance mechanisms have similar structure.

Weak features corresponding to ν_4 of the guests have been observed in some mixed crystals. The spectra are summarized in table 7. To help with the analysis, data of ReF_6 in TeF_6 have also been included. Performing a calculation similar to that for the ν_5 vibrations in mixed crystals based on eqs. 12, estimates of pseudoresonance shifts are greater than 10 cm^{-1} WF_6 in UF_6 and less than 1 cm^{-1} for UF_6 in WF_6.

Table 7
Summary of the observed ν_4 Raman spectra in dilute mixed crystals

Guest	Host	Frequency (cm^{-1})	FWHH (cm^{-1})	Relative intensities	Center of gravity (cm^{-1})	Gas-to-crystal shift (cm^{-1})
WF_6	UF_6	250.45	2.6	2		
		267.45	1.3	1	256.05	+4.0
UF_6	WF_6	168.91		1		
		173.47	2.6	2	171.95	−14.2
ReF_6	TeF_6	246.81	2.8	2		
		250.71		1	248.11	−8.9

Scatter of the centers of gravity is again both a static and a pseudoresonance effect, the latter being suggested to be more important. No detailed explanation is known for the increased site splitting of WF_6 in UF_6. Perhaps selective pseudoresonance rather than just static interactions are responsible. A reasonable estimate of the ν_4 gas-to-crystal shift for an ideal mixed crystal is between -15 cm^{-1} and -5 cm^{-1}. These negative values fall into the scheme presented in the last section where the static site shifts due to crystal induced Fermi resonances would shift ν_5 upward and ν_4 downward.

The comments about MoF_6 isotope effects for the ν_3 vibration apply to ν_4. For $^{92}MoF_6$ and $^{100}MoF_6$ the gas phase frequencies [14] are 265.7 and 262.7 cm^{-1}. Scaling the isotopic splitting by the width of the exciton band, these differences are seen to be comparable to those found for the ν_3 band. Again, resonance interactions dominate the site identities of these species.

The most important observations for ν_4 bands are: (1) the bands are similar in all systems; (2) they are dipolar in nature; (3) the band width ratios for ν_3/ν_4 for each crystal scale semiquantitatively with the gas phase ν_3/ν_4 oscillator strength ratios; and (4) gas-to-crystal shifts involve crystal induced Fermi resonance and pseudoresonances, as occurred with ν_5, in this crowded spectral region.

4.6. ν_6 bands

The ν_6 bands were the weakest fundamental transitions observed; consequently only neat crystal spectra were obtained. Table 8 lists the vapor phase frequencies of ν_6 (derived from combination and overtone transitions) and $2\nu_6$ transitions (observed in Raman) [14–16] along with the observed crystal transition frequencies. The crystal values are only (a part of) the $k = 0$ structure. Even so, the centers of the $2\nu_6$ structures are nearly harmonic with respect to the centers

Table 8
ν_6 and $2\nu_6$ frequencies

Molecule	ν_6 frequency (cm^{-1})		$2\nu_6$ frequency (cm^{-1})	
	vapor [a]	crystal (this work)	vapor [b]	crystal (this work)
MoF_6	117	140	233	278.2
WF_6	129	147	255	291.4
UF_6	143	145.8 149.0 155.3 163.3	281	308.4

[a] Derived from combinations and overtones (refs. [14–16]).
[b] Observed Raman transition frequencies (refs. [14–16]).

of the observed ν_6 features. In the absorption spectra of ReF_6 in these host crystal [3], the corresponding two-particle bands are approximately centered around 144, 155 and 158 cm^{-1} in MoF_6, WF_6, and UF_6. These values for ν_6 might be true indicators of the band centers or they might reflect the mixing of single particle and two-particle states. Regardless, it is clear that a sizeable positive gas-to-crystal shift has occurred. These shifts are especially large when considered with respect to the absolute frequency of ν_6.

Consider the effect of adding a perturbing quadratic (crystal) potential energy term to a harmonic oscillator so that its frequency increases from ν to $(1+x)\nu$. The effect of adding the same potential to an oscillator of frequency $a\nu$ is to raise it to $\approx(1 + x/a^2)a\nu$. A shift of $x\nu$ in the original oscillator corresponds to a shift of $\approx(x/a)\nu$ in the other when the *same* additional quadratic potential is applied. This effect is observed in the gas-to-crystal shifts of the series MoF_6, WF_6, and UF_6. However, exact agreement would require (besides more accurate experimental data) consideration of the variation of reduced masses and differences of crystal potentials.

This analysis seems rather ad hoc in view of the consistent previous discussions of large gas-to-crystal shifts associated with crystal induced Fermi resonance. It may well be, however, that the crystal potential function projects preferentially or disproportionately onto the ν_6 (t_{2g}) octahedral coordinate. Nonetheless, the trends in the gas-to-crystal shifts ($MoF_6 > WF_6 > UF_6$) are also consistent with a substantial $\nu_4-\nu_6$ Fermi resonance in UF_6. It is likely that both Fermi resonance and the previous potential function arguments are responsible for the total gas-to-crystal (albeit neat crystal) behavior.

5. Evaluation of the transition multipole interaction model

Table 9 is a summary of the excitonic interaction mechanisms based on electrostatic multipolar models for the various bands and a comparison of their magnitudes in the various crystals. As discussed in ref. [3], all crystals have very nearly identical crystal dimensions. The trend of the dipolar band widths, which are larger than the other bands, are followed semiquantitatively by the infrared transition intensities.

The quadrupolar bands have been fit with a calculation. A sizeable part of the distinction between the UF_6 and the WF_6, MoF_6 sets of interactions stems from the larger amplitudes of vibration, the larger metal–fluorine distances, and hence the large derivatives of the polarizability [10]. A point charge model would require partial fluorine charges of 0.62 in the WF_6, MoF_6 set and 0.80 in UF_6 to fit the ν_2 band widths. These values then predict ν_5 band widths of 8.9 and 28 cm^{-1}. A static model is too simple, though. Electronic charge polarization is undoubtedly important during nuclear displacements and is probably more important for UF_6 than for WF_6 and MoF_6. A greater electronic polarizability for UF_6 is not inconsistent with, for instance, the smaller UF_6 ν_3 band width compared to that of MoF_6. The central metal

Table 9
Summary of band parameters and electrostatic excitonic mechanisms

Vibrations	Approximate bandwidths (cm^{-1})			Apparent excitonic mechanisms (first non-vanishing electric multipolar moment)
	MoF_6	WF_6	UF_6	
ν_1	$\lesssim 1$	$\lesssim 1$	$\lesssim 1$	hexadecapolar and crystal induced lower transition moments
ν_2	10.0	9.7 a)	23.6	quadrupolar
ν_3	≈ 70 b)		≈ 65	dipolar
ν_4	24	26	26 b)	dipolar
ν_5	8.7	8.0	22.9	quadrupolar

a) Mixed strongly with ν_3 band
b) Extrapolation of observed structure onto more completely observed bands of other crystals.

moves in this mode so that greater relative motion of charge centers occurs for the molecule with lighter metal (MoF_6). The greater motion must be balanced against the difference in electronic polarizabilities to give the approximately equal dipole derivatives (or exciton bands).

Ionicity of transition metal hexafluorides has been discussed and found to be necessary for treatment of vibrational force fields [22,23]. In fact, in a recent series of Xα calculations of UF_6 electronic properties [24], a crude population analysis of the results placed a charge of −0.27 on each fluorine. Examination of the electron density plots for PtF_6, determined also via Xα calculation [25], shows that the charge distribution on the central metal is increased along the bonds and there is also significant density blossoming outward from the fluorine nuclei (on the same axes). These factors would increase the effective quadrupole moment above that of a point charge assignment.

This discussion should not be construed as proof of the adequacy of the multipolar model; it does, however, support it. It would be interesting to perform the dipolar calculation and compare parameters. At some level the finer points of the atom–atom interactions must be included (although formally they could be projected onto higher multipolar interactions). The ν_6 bands would have (if the molecules were perfect octahedra) an octupole–octupole term as the first nonvanishing interaction. It would be quite a test to see what molecular parameters would be required to fit the ≈ 18 cm^{-1} band of UF_6 with this presumably weaker interaction.

6. Conclusions and summary

The vibrational exciton bands of MF_6 (M = Mo, W, U) have been investigated through the Raman spectra of neat and mixed crystals. Site energies (gas-to-crystal shifts), $k = 0$ structure, $k \approx 0$ dispersions, and the densities of states have been examined using fundamental band neat and mixed crystal spectra, two-particle ($\nu_1 + \nu_i$) neat crystal spectra, and ν_2 and ν_5 quadrupole–quadrupole calculations as sources of information.

The individual neat crystal bands have been understood in terms of electrostatic multipole models with the scaling between crystals or bands of the same crystal being reasonably consistent with molecular parameters (dipole derivatives, partial charges, bond distance, amplitudes of vibration, electronic polarizability).

In discussing site energies (or band centers) and intensities of Raman spectra, crystal induced Fermi resonances were found to be important. The ν_6 mode evidenced the effects of additional potential energy terms on a low energy vibration.

In discussing dilute mixed crystals it becomes apparent that pseudoresonances were important. This appears somewhat at odds with the fact that the band structures are relatively independent of the compound and its exact distribution of vibrational energy levels and resonance mechanisms. It may be that the interaction between bands is partially projected onto a band center shift term. Such overall band shifts can be incorporated quite nicely into a general crystal induced Fermi interaction. The remaining differential shift terms, which change relative $k = 0$ positions, may be small. These interactions which appear most prominently in the bending region, may be associated with the inability to obtain an accurate fit of the calculated ν_5 $k = 0$ structure with that observed for UF_6 (most clearly resolved). A good fit to the ν_2 bands of MoF_6 and UF_6 is obtained with the same quadrupolar calculation.

The concept of the ideal mixed crystal has been shown not to be rigorously correct for the mixed crystal vibrational properties of MoF_6 or WF_6 with UF_6.

References

[1] E.R. Bernstein and G.R. Meredith, Chem. Phys. 24 (1977) 289.
[2] E.R. Bernstein and G.R. Meredith, Chem. Phys. 24 (1977) 301.
[3] E.R. Bernstein and G.R. Meredith, J. Chem. Phys. 64 (1976) 375.
[4] E.R. Bernstein and J.D. Webb, Mol. Phys., to be published.
[5] R. Kopelman, Excited states, Vol. 2, ed. E.C. Lim (Academic Press, New York, 1975) p. 34 ff.
[6] M.R. Philpott, Advan.Chem. Phys. 23 (1973) 228.
[7] G.W. Robinson, Ann. Rev. Phys. Chem. 21 (1970) 429.
[8] A.S. Davydov, Theory of molecular excitons (Plenum, New York, 1971).
[9] E.R. Bernstein and G.R. Meredith, J. Chem. Phys., to be published.

[10] G.R. Meredith, Thesis, Princeton University (1977).
[11] V.N. Prusakov and U.K. Ezhov, At. Energ. 25 (1968) 64 (in: Chem. Abs. 69 (1971) 70402f).
[12] J.J. Barghusen, Power Reactor Technol. Reactor Fuel Process 10 (1966–7) 70 (in: Chem. Abs. 68 (1971) 83440w).
[13] G.R. Meredith, J.D. Webb and E.R. Bernstein, Mol. Phys., to be published.
[14] R.S. McDowell, R.J. Sherman, L.B. Asprey and R.C. Kennedy, J. Chem. Phys. 62 (1975) 3974.
[15] R.S. McDowell and L.B. Asprey, J. Mol. Spectry. 48 (1973) 254.
[16] R.S. McDowell, L.B. Asprey and R.T. Paine, J. Chem. Phys. 61 (1974) 3571.
[17] T.G. Burke, D.F. Smith and A.H. Nielsen, J. Chem. Phys. 20 (1952) 447.
[18] H.H. Claassen, G.L. Goodman, J.H. Holloway and H. Selig, J. Chem. Phys. 53 (1970) 341.
[19] G. Friedlander, J.W. Kennedy and J.M. Miller, Nuclear and radiochemistry (Wiley, New York, 1964).
[20] H.H. Claassen, H. Selig and J.G. Malm, J. Chem. Phys. 36 (1962) 2888.
[21] B. Frlec and H.C. Claassen, J. Chem. Phys. 46 (1967) 4603.
[22] H. Kim, P.A. Souder and H.H. Claassen, J. Mol. Spectry. 26 (1968) 46.
[23] N. Thakur and D.K. Rai, J. Mol. Spectry. 19 (19) 341.
[24] M. Boring and J.W. Moscowitz, Chem. Phys. Letters 38 (1976) 185;
B. Schneider, A.M. Boring and J.S. Cohen, Chem. Phys. Letters 27 (1974) 577;
M. Boring, J.H. Wood and J.W. Moskowitz, J. Chem. Phys. 61 (1974) 3800.
[25] J.T. Waber and F.W. Averill, J. Chem. Phys. 60 (1974) 4466.